

KINETICS OF ELECTRON TRANSFER REACTIONS IN HYDROTHERMAL AND SUPERCRITICAL WATER*

Jason A. Cline, Kenji Takahashi,[†] Timothy W. Marin,
Charles D. Jonah, and David M. Bartels
Argonne National Laboratory, Chemistry Division
9600 S. Cass Ave., Argonne, IL, 60439

ABSTRACT

The rates of several radiation-induced reactions are assessed via pulse radiolysis in order to extend a model for nuclear reactor coolant radiolysis to supercritical conditions. We find changes in radiolysis yields and significant deviations from Arrhenius behavior at 250 bar as the temperature approaches and exceeds the critical temperature of pure water. At 380°C we also observe a strong pressure dependence of the reaction rates of ions and hydrophobic species. Using a homogeneous chemistry model, we find by 350°C that the relatively mild changes in these reaction rates increase the predicted critical hydrogen concentration relative to 325°C.

INTRODUCTION

Corrosion and nuclear power

In any coolant loop with its crevices, dissimilar metals, and contaminants there will be issues of materials performance, and nuclear power is no exception. The working fluid of a nuclear power plant is commonly water, which also has moderating capabilities. Materials performance is very important in nuclear systems not only because of the high reliability required, but also because it is desirable to limit the mobility of “activated” radioactive metals, which could be transported as aqueous hydroxides or oxide scales. In conventional power plants this is a matter of thermodynamics. For example, if the oxidation potential of the coolant solution is sufficiently reducing, the metals will be stable (neglecting galvanic action). Nuclear plants have the additional factor that the water is exposed to ionizing

* Work performed under the auspices of the Office of Basic Energy Sciences, Division of Chemical Science, US-DOE under contract number W-31-109-ENG-38.

[†] Present address: Division of Quantum Energy Engineering, Hokkaido University, Sapporo 060-8628, Japan.

radiation. This can produce as stable molecular products hydrogen, oxygen, and hydrogen peroxide as well as possibly influencing the pH of the system.

Radiation chemistry of water

When ionizing radiation (beta particles, gamma photons, neutrons) strikes water, energy is deposited into all of the quantized electronic and nuclear degrees of freedom of the H₂O molecules. For (low LET, or Linear Energy Transfer) beta and gamma radiation, the mechanism is primarily scattering into the electronic energy levels. The largest cross-sections are for processes that initially produce low energy (20–100 eV) secondary electrons and (H₃O⁺, OH) pairs. The secondary electrons produce secondary ionizations, and eventually become solvated electrons (e⁻)_{aq}. The clusters of primary and secondary ionization events are called “spurs”, and the low-LET radiation essentially leaves behind a track of well-separated “spurs”. In contrast, neutrons are stopped by the hydrogen or oxygen nuclei, and all of the energy is converted to kinetic energy of these recoil ions. The recoil ions produce very dense cylindrical tracks of radiolysis products, and the (high LET) chemistry is qualitatively different due to the extremely high density of reactive fragments.

Some fraction of the species created in spurs or in dense tracks escape into the bulk fluid by diffusion, where they participate in homogeneous chemistry. These radiolysis yields are quantified in terms of a “G-value” or number of molecules per 100 eV of energy. Because they result from the non-homogeneous recombination chemistry, G values depend on water temperature and density, and on particle or photon mass and energy. Whereas the initial G-values for low LET gamma and beta radiation is dominated by free radical fragments, low LET neutron radiation produces essentially all molecular hydrogen, oxygen, and hydrogen peroxide.

The species that are produced by the radiolysis include: (e⁻)_{aq}, H⁺, HO₂⁻, H, OH⁻, OH, HO₂, H₂, O₂, and H₂O₂. These species participate in a network of many reactions to yield stable ions and molecular species. It is the oxidizing species O₂ and H₂O₂ which are of greatest concern, for these will bring the electrochemical potential in the reactor to a level higher than desired, and allow oxidation of the process plumbing and the development of crud (various oxides and/or hydroxides) deposits. Molecular oxidizing species are developed in recombinations of OH and HO₂ radicals:



Unfortunately direct measurement of the concentrations of these species in the reactor core is difficult to impossible. One can only monitor concentrations in samples taken from locations which are out-of-core, and this does not provide a high-fidelity picture of the chemical environment of the core. Thus to truly understand the in-core chemistry relevant to corrosion we must develop a comprehensive model of the coolant’s radiation chemistry. This approach is particularly important when considering operating conditions where operational experience is lacking.

Supercritical water coolant

The application of interest is just such a condition: a supercritical-water-cooled nuclear reactor. Through experiments and operational experience it has been well-established that a solution to the problem of water radiolysis under normal (T ≤ 300°C) temperatures is an initial charge of excess hydrogen. This solution exploits the reactions:



which convert the oxidizing species to reducing species at a rate sufficient to suppress net production of O₂ and H₂O₂. As water-cooled nuclear power plants increase reactor temperature to improve their achievable (Carnot) efficiency, they surpass the critical temperature of water. Some designs under

consideration employ a pressure of 250 bar, which is above the 221 bar critical pressure for pure water. Thus the water undergoes a continuous change from a subcritical liquid to supercritical fluid.

The sub- to supercritical water transition involves dramatic solvent property changes which are expected to affect the radiolysis yields and reaction rates. Along the isobar of 250 bar, as the temperature increases from room temperature, density slowly decreases, then dramatically decreases in the vicinity of the critical temperature (374°C). Ion product of water is the largest at about 250°C, and falls rapidly above 350°C as the drop in static dielectric constant overwhelmingly encourages ions to reassociate. With such large and abrupt changes in solution properties there are some very legitimate concerns as to whether the understanding of radiolysis gained from lower-temperature measurements may be extrapolated to the supercritical system. Below we find that some reactions which can be well described with Arrhenius parameters up to 300°C change dramatically as we approach and surpass the critical point of pure water, and that yields are also subject to dramatic changes.

Radiolysis Model

The full complement of reactions, equilibria, and radiolysis yields known to be relevant to water radiolysis up to 300°C was compiled by Elliot.¹ Despite its comprehensive nature, Elliot points out that there are still many parts of the model which are supported by few data or solely by extrapolations. In this work we attempt with new measurements to build on this model framework for an eventual goal of a comprehensive radiation chemistry model.

EXPERIMENT

To begin to extend the radiolysis model, we have examined some reactions from lower (100°C) temperatures to supercritical conditions (400°C). Using pulse radiolysis techniques with transient absorption spectroscopy of the solvated electron (e^-_{aq}), we measured directly the rates of several reactions in sub- and supercritical water. The details of the experimental method are published elsewhere^{2,3} but we briefly summarize them now. We have a specially-designed high-pressure and temperature optical cell positioned on an electron accelerator beamline. A supercritical water solution is slowly flowed through the optical cell where we dose it with short (4 ns) pulses of 20 MeV electrons. As stated above, the irradiation pulse creates many species (according to low linear-energy-transfer yields) one of which is the solvated electron (e^-_{aq}). The solvated electron absorbs light from our pulsed Xe arc lamp light source. We detect this absorbance as a function of time and thus track the solvated electron concentration (Figure 1). By changing the solution composition and doses we can measure reaction rates.

RESULTS

Ion-Hydrophobe Interactions: Reactions of (e^-_{aq}) with S7 and O₂, and the reaction (H + OH⁻)

The first class of reactions which we evaluated were reactions of ions with hydrophobic species. We evaluated the reaction rates of the hydrated electron (e^-_{aq}) with oxygen in neutral water.



In a separate experiment, reactions of (e^-_{aq}) with S7 and a competing reverse reaction were measured in mildly alkaline (10⁻³ m KOH) solution:



(While S7 is not a component of reactor cooling water, it is a hydrophobic electron scavenger which allows us to elucidate Reaction (8) without etching our sapphire windows, as would happen under alkaline conditions with oxygen.) We found in each of these reactions that, up to 300-350°C, their rate constants increased with temperature in an Arrhenius or, for Reaction (8), nearly-Arrhenius fashion. However, above this range, the effects of the solvent changed the temperature dependence, such that the rate actually dipped quite significantly at about 380°C (Figures 2 and 3). In the O₂ data, in which we exceed 380°C, we find that the dip is peculiar to 380°C; at 400°C the rate constant is seen to resume its upward climb. We ascribe this observation to the changing structure of the water, which may hinder electron transfer at points where electrostriction and enhancement of local coordination number around solvated ions is strongly favored.

A second effect which cannot be ignored is the density effect in the supercritical fluid (Figure 4). We find for these three reactions at 380°C that their rate constants are affected by the solvent density. See Ref. [2] for more discussion.

Low-LET yield ratio of H to (e⁻)_{aq}

From the absorbance traces in Reactions (7) and (8) we were able to deduce the initial ratio of (e⁻)_{aq} to H atom (Figure 5). Our results for higher temperatures showed a surprising increase in this initial radiolysis yield of H atom relative to (e⁻)_{aq} for fast-electron irradiation as density decreased. This effect was not significant below 350°C, but was very significant at the maximum temperature investigated, 380°C.

Figure 6 shows the density-normalized peak intensity of the hydrated electron absorption at 380°C in 0.3×10⁻³ mol·kg⁻¹ KOH solution. If we assume that the absorption coefficient of (e⁻)_{aq} is constant at 380°C, and that electron beam stopping powers are proportional to density, then we find that the yield of (e⁻)_{aq} is increasing at lower densities, and the yields of H are consequently increasing even more dramatically.

Self-reaction of (e⁻)_{aq}

The self-recombination reaction of solvated electrons with themselves and water



was measured under hydrogen up to 325°C. These preliminary results show qualitative agreement with the previous work of Christensen and Sehested.⁴ The second order recombination rate increases with an Arrhenius behavior up to 150°C, but then decreases dramatically. We have extended the measurements to somewhat higher temperatures, where we find that the rate at high temperatures eventually increases again (Figure 7).

The reaction H⁺ + (e⁻)_{aq}

Reactions of the solvated electron with protons



were measured using perchloric acid solutions up to 350°C. Our preliminary measurements support the non-Arrhenius behavior measured by Shiraishi et al.⁵ and extend it to 350°C (Figure 8), both of which disagree with AECL's Arrhenius fit.¹

EXTENSION OF RADIOLYSIS MODEL

Having performed these measurements and observed some trends in behavior for various classes of reactions, we find that direct measurement of different classes of reactions under controlled conditions is crucial for proper understanding of the chemistry at these elevated conditions. The region of (*P*, *T*) space

which is most interesting to the application lies along the 250 bar isobar and spans a wide range of temperatures. Because the data are limited, we chose to parameterize all predictions for pressures of 250 bar, where we have the most data and also the highest degree of applicability to conditions which are currently considered for future SCW-cooled nuclear reactor designs.

The 350°C “confidence barrier”

While our ion-hydrophobe reactions are measured up to 400°C, most of our other measurements so far extend only to 350°C. This is also the limit for the reliable calculation of free energies of such species as HO_2^- and H_2 within SUPCRT92,⁶ which aided in our extension of some of the high-temperature equilibria. Further, there are many other classes of reactions whose behavior near the critical point of water has not been assessed. We therefore must relegate extension of the radiolysis model above 350°C to future work. Below we present our adaptations of our new data to the radiolysis model.

Data for which we have not developed a theoretical model or a simple Arrhenius fit were entered into the model using splines. Reaction categories for which we had more information on general behavior were applied more broadly.

Reactions of ions and hydrophobic species

Reactions of hydrated ions and hydrophobic species, $(e^-)_{\text{aq}} + \text{O}_2$, $(e^-)_{\text{aq}} + \text{S7}$, and $\text{H} + \text{OH}^-$ exhibit definite parallel trends in their behavior at high temperatures. The S7 and O_2 reactions most notably follow the Arrhenius relation at lower temperatures (the $\text{H} + \text{OH}^-$ reaction deviates from its low-temperature activation energy above 100°C), then deviate from it in the same way at high temperatures. The functionality of the rate constants with density at 380°C is also parallel. Using the O_2 reaction at 250 bar as the standard, the function of deviations from Arrhenius behavior was factored out. This function was then applied to the other ion-hydrophobe reactions in the model.

Equilibria

Water self-ionization pK_W was parameterized for 250 bar from the data of Marshall and Franck.⁷ The pK_a 's of OH^- and H_2O_2 , which are assumed to track pK_W above 200°C (where the data stop) were brought into conformance with the new parameterization.

pK_a of H atom was extended using data of Shiraishi et al⁵ with solvation data for H^+ and H derived from SUPCRT92. H atom solvation is not specifically treated by SUPCRT92; we estimated its energy by assuming that the solvation energy of the hydrophobic species H_2 and H are the same, and accounting for the change in the energy of formation of the two.

Similarly, the reaction equilibrium constant for the reaction



was treated to 350°C using calculations at 250 bar from SUPCRT92.

For lack of data pK_a of HO_2 radical was left unchanged.

DISCUSSION

None of the new data, except for reaction (8), show significant deviations at 300°C or below from the older data. However, the implications for higher temperatures is very clear: the reactions and yields are significantly affected. To 350°C, Reactions (7), (8), and (9) show significant deviations from the trends one might have inferred from lower temperatures. At still higher temperatures, the ion-hydrophobe reactions (6) through (8) drop near 380°C in a common manner. At decreased density the fast-electron irradiation yield of H relative to $(e^-)_{\text{aq}}$ is increased many times over.

While the changes are much more dramatic at 380°C we do not yet have enough information to construct a meaningful prediction for the full reaction network. However, we can assess the effects at up to 350°C under 250 bar pressure. To see this we examine critical hydrogen concentration.

Trends in critical hydrogen concentration

A measure which is important to industrial applicability is the critical hydrogen concentration (CHC). This is defined as the initial hydrogen concentration required in the coolant which balances net hydrogen production. Adding a surplus of hydrogen will cause elevated hydrogen concentrations, while initial hydrogen concentrations below the CHC do not sufficiently suppress radiolysis, and as such the hydrogen is consumed. Hydrogen suppresses oxygen and peroxide production by reacting with OH radicals to produce H radicals and water. The H radicals then react with H₂O₂ to reproduce OH radicals and water. When hydrogen is absent, H₂O₂ reacts with OH radicals to produce HO₂ radicals and water; pairs of HO₂ radicals then can react to form oxygen and H₂O₂.

We compute the CHC for various temperatures at 250 bar with a dose rate of 2400 Gy/s, where 30% of the dose is from low-LET irradiation (β , γ) and the balance is from neutrons. Figure 9 shows the trends in CHC from the earlier model and the model enhanced with our new data. The CHC are nearly identical approaching 325°C, but in the enhanced model the CHC *increases* between 325 and 350°C. This corresponds in fact to the points where the new reaction data diverge from the older data. As it is known⁸ that this pure-water homogeneous chemistry model tends to underpredict the true CHC, the results of these calculations should be viewed in terms of trends rather than absolute values.

SUMMARY

The rates of several homogeneous (bulk phase) radiation-induced reactions were measured in hydrothermal and supercritical water. We find that their rate constants depart significantly from trends inferred from lower temperatures. Preliminary estimates indicate that instead of steadily dropping, the critical hydrogen concentration required to suppress radiolysis turns around and begins to increase.

ACKNOWLEDGEMENTS

This work was performed under the auspices of the Office of Basic Energy Sciences, Division of Chemical Science, US-DOE under contract number W-31-109-ENG-38. It was also partially funded by the Nuclear Energy Research Initiative (NERI). The authors thank Craig Stuart and David McCracken of AECL for providing many helpful resources.

REFERENCES

- 1 A.J. Elliot, "Rate Constants and G-Values for the Simulation of the Radiolysis of Light Water over the Range 0–300°C," Report AECL-11073, Atomic Energy of Canada, Limited, October 1994.
- 2 J. A. Cline, C. D. Jonah, and D. M. Bartels, "Pulse Radiolysis of Supercritical Water I. Reactions Between Hydrophobic and Anionic Species," submitted to J. Phys. Chem. A, Oct. 2001.
- 3 K. Takahashi, J. A. Cline, D. M. Bartels, and C. D. Jonah, "Design of an Optical Cell for Pulse Radiolysis of Supercritical Water," Review of Scientific Instruments, 71(9):3345 (2000).

- 4 H. Christensen and K. Sehested, "The Hydrated Electron and its Reactions at High Temperatures," *J. Phys. Chem.*, 90:186 (1986).
- 5 H. Shiraishi, G. R. Sunaryo, and K. Ishigure, "Temperature Dependence of the Equilibrium and Rate Constants of Reactions Inducing Conversion Between Hydrated Electron and Atomic Hydrogen," *J. Phys. Chem.* 98:5164 (1994).
- 6 J. W. Johnson, E. H. Oelkers, and H. C. Helgeson, "SUPCRT92: A software package for calculating the standard molal thermodynamic properties of minerals, gases, aqueous species, and reactions from 1 to 5000 bar and 0 to 1000°C", *Computers and Geosciences*, 18(7):899 (1992).
- 7 W. L. Marshall and E. U. Franck, "Ion product of water substance 0–1000°C, 1–10,000 bars," *J. Phys. Chem. Ref. Data*, 10(2):295 (1981).
- 8 D. R. McCracken, K. T. Tsang, and P. J. Laughton, "Aspects of the Physics and Chemistry of Water Radiolysis by Fast Neutrons and Fast Electrons in Nuclear Reactors," Report AECL-11895, Atomic Energy of Canada, Limited, September 1998.
- 9 K. D. Asmus and J. H. Fendler, *J. Phys. Chem.*, 72:4285 (1968).

FIGURES

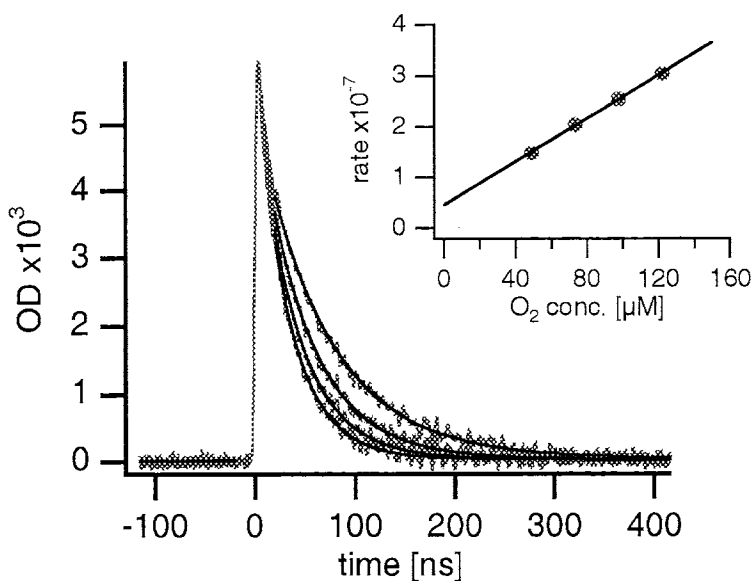


FIGURE 1: Sample fitted data and pseudo-first-order plot for scavenging of solvated electrons by O_2 . The conditions were 370°C and 204 bar, in the subcritical vapor phase (0.165 g/cc).

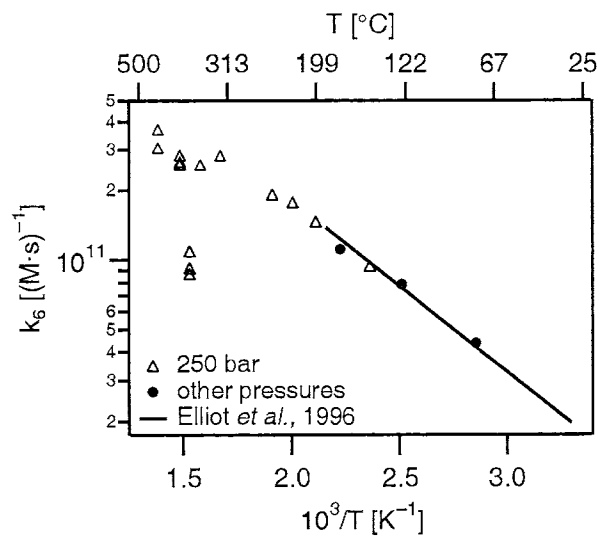


FIGURE 2: Arrhenius plot of reaction (6) $\text{O}_2 + (\text{e}^-)_{\text{aq}}$ at 250 bar and lower pressures, compared to existing literature.¹ The rapid dip in rate at 380°C illustrates the effect of the compressible solvent on the reaction rate.

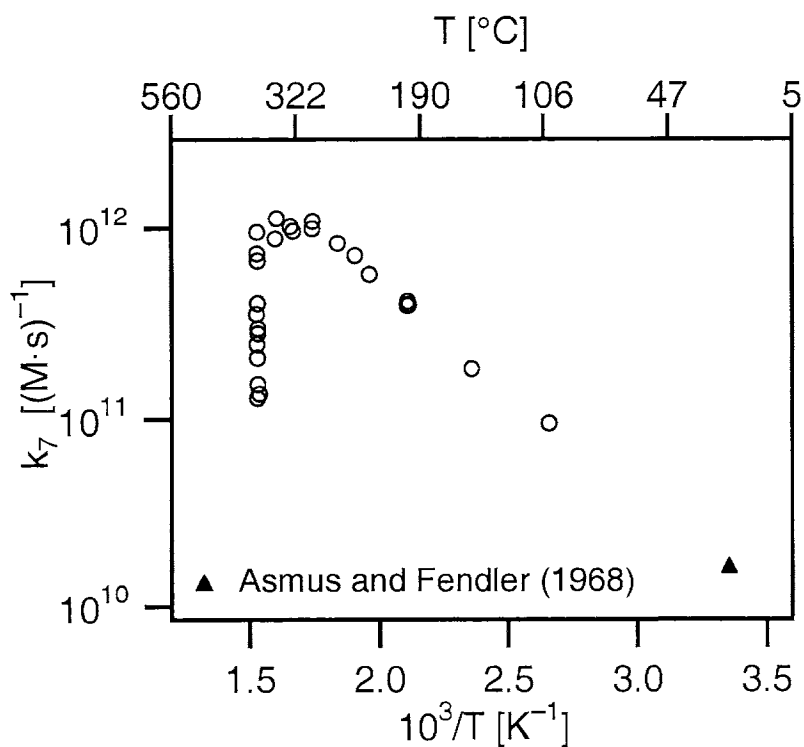


FIGURE 3 Arrhenius plot for reaction (7). The leftmost data are for 380°C at various pressures. Published data are from Ref. [9].

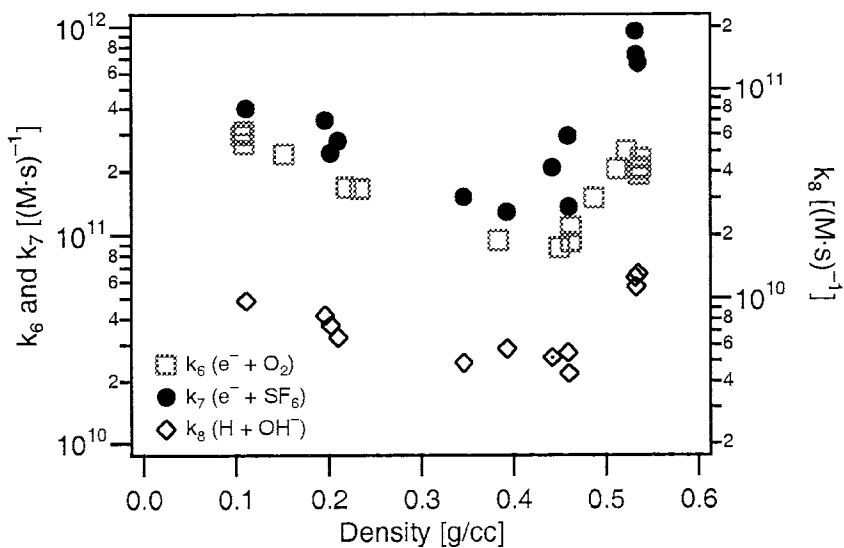


FIGURE 4: Density dependence of reactions (6) through (8) at 380°C. Note the log scale for k_8 (right side) is shifted for easy comparison with the other reactions.

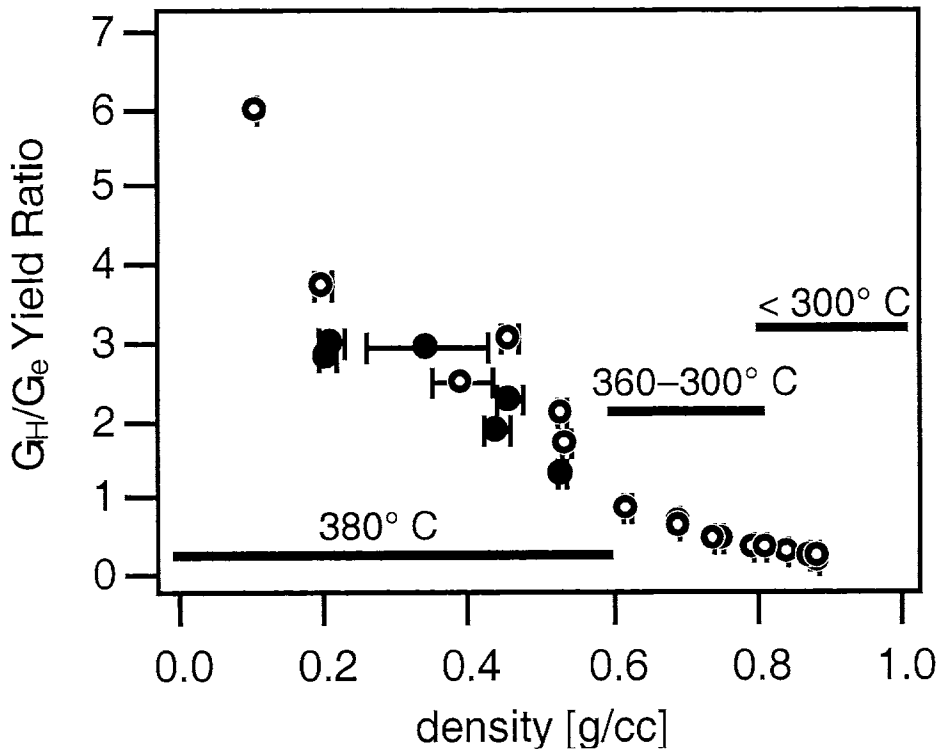


FIGURE 5: Change of apparent yield ratio G_H/G_e with solution density. Above $\rho=0.6$, density is chiefly governed by temperature.

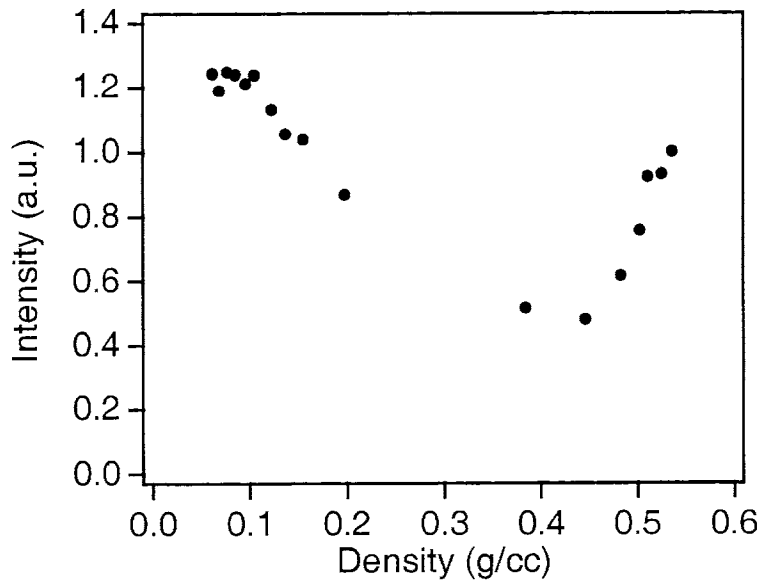


FIGURE 6: Dose-normalized absorption intensity at 380°C as a function of solution density.

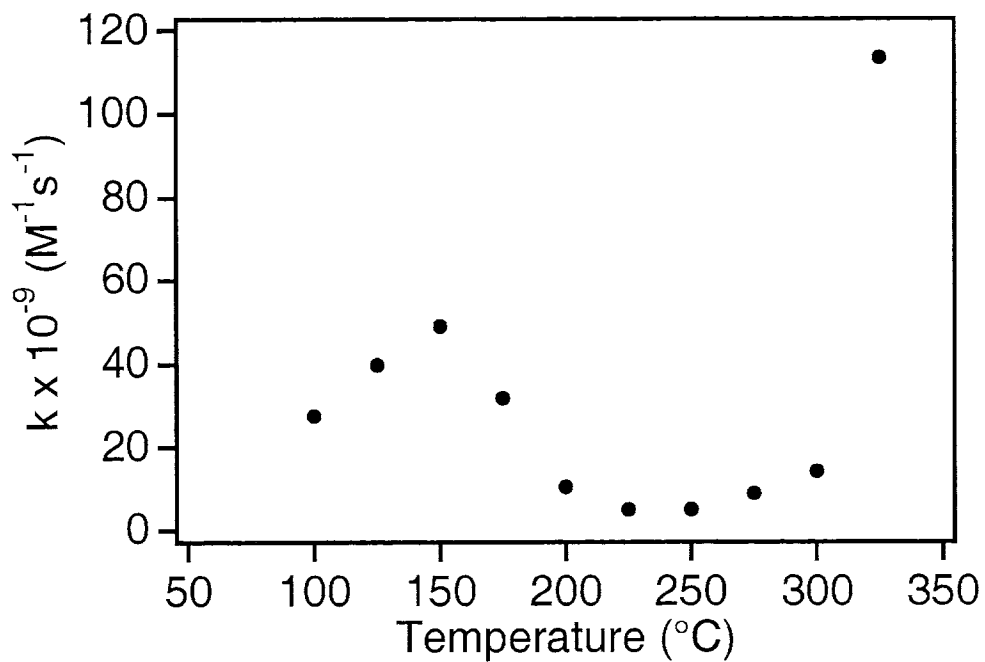


FIGURE 7: Bimolecular rate constant for reaction (9), the self-recombination of $(e^-)_{aq}$.

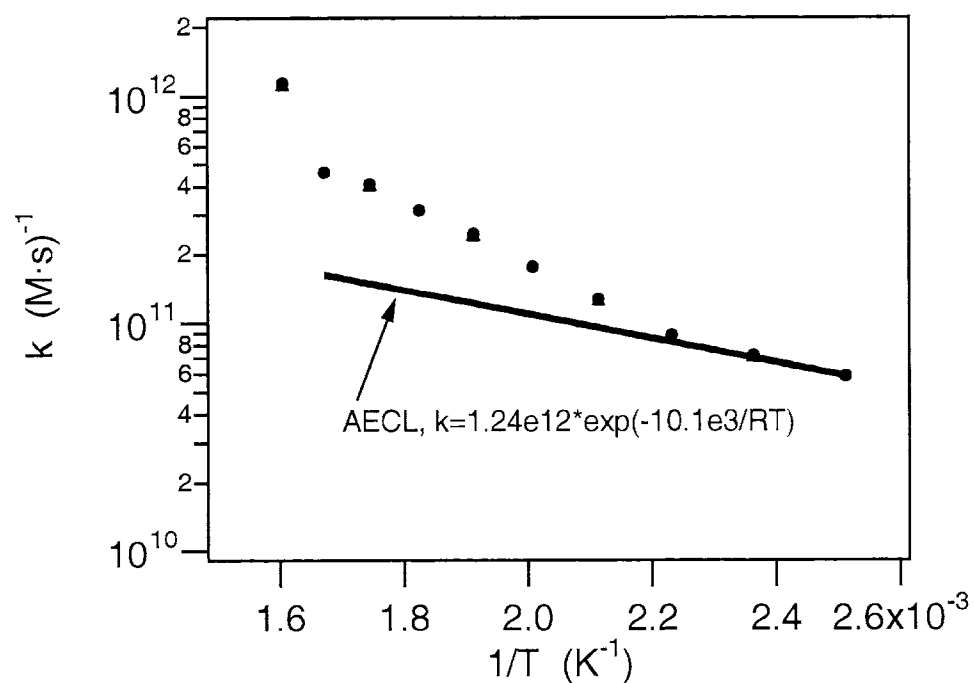


FIGURE 8: Measured rate constant for reaction (10), of $(e^-)_{aq}$ with H^+ , contrasted against published values.¹

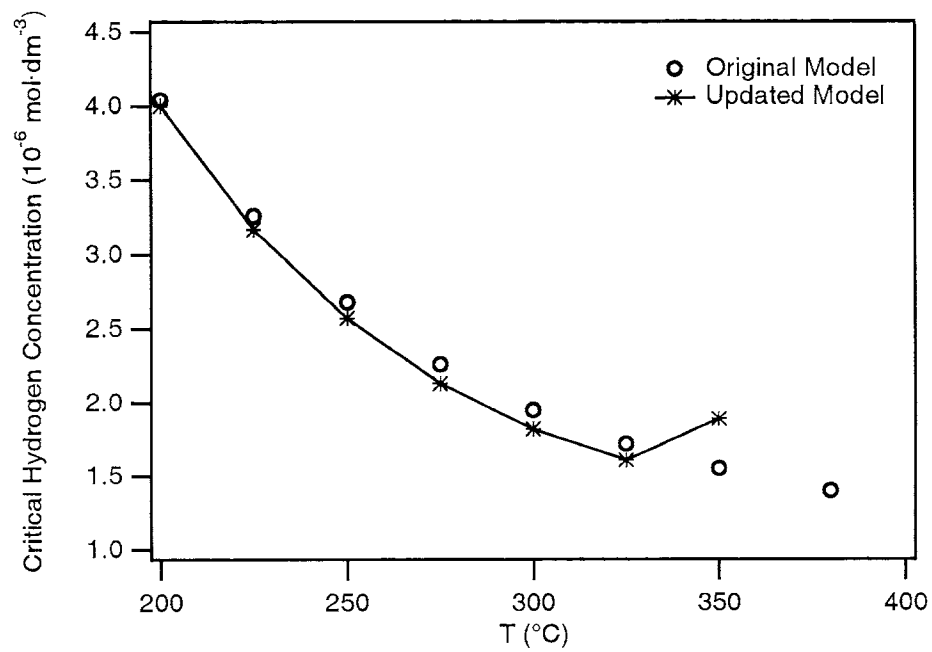


FIGURE 9: Critical hydrogen concentration computed at 250 bar for various temperatures.